Optically Transparent Single-Layer Microwave Metamaterial Absorber

Furkan Şahin, Emre Ünal, Vakur B. Ertürk, and Hilmi Volkan Demir

***Abstract*—Recent advances in metamaterials have allowed to impart unique properties to flat RF absorbers, including broadband absorption, low thickness (in terms of the longest operating wavelength, λ_L), polarization insensitivity, and optical transparency. However, achieving all of these critical characteristics in a single design is a challenging task. Here, we propose and demonstrate an optically transparent and extremely thin metamaterial absorber (with a thickness of $0.079\lambda_L$) made of a single layer of polymethyl methacrylate (PMMA) as the substrate and the indium-tin-oxide films as the ground plane and the patterned layer on top of the PMMA layer. The fabricated prototypes exhibit over 90% absorption between 4.4 GHz and 11.2 GHz and over 95% absorption between 4.8 GHz and 10.6 GHz without any air-gaps. Furthermore, the absorber is insensitive to polarization and provides more than 90% absorption for incident angles up to 60° for transverse magnetic, and 40° for transverse electric polarizations without any compensation layer requirement. Besides RF characterizations, we optically recorded the transmittance in the visible range to be 65% on average for the tested absorbers. The proposed architecture holds great promise for use in stealth air plane canopies due to extended 95% absorption while offering reduced fabrication cost.**

***Index Terms*—Absorber, metamaterial, optically transparent, pixelated.**

I. Introduction

METAMATERIALS are human-made structures capable of modifying the electromagnetic properties of materials to impart a variety of unique features, for instance, considerably improved electromagnetic absorption over a wide frequency range while being flat [1]. Moreover, metamaterials allowed absorbers to achieve further properties, such as broadband absorption, small thickness in terms of operating wavelength, polarization, and oblique incidence insensitivity. However, achieving all the abovementioned properties together has been a pending problem, and extensive research was conducted to find desired absorber structures [2]. Diverse absorber designs that possess broadband absorption with a minimum thickness were studied in the form of multilayer structures [3], [4] and multiple scaled versions of the same geometry within the unit cell [5], [6], introducing lumped elements [7], [8], and combining multiresonant structures [9], [10], [11]. Circuit analog absorbers (CAAs) can be considered multiresonant structures that combine resistive sheets with reactive components due to straight parts and gaps between elements. CAAs can achieve wider bandwidths with a minimum thickness [12]. Furthermore, geometry tailoring or pixelation of geometrical shapes of CAAs to attain different designs was presented in [13]. On the other hand, polarization insensitivity and wide-angle stability are desired metrics for absorbers as reported in [14], [15], [16], and [17]. Recently, metamaterial designs with optically transparent materials have been investigated and several applications can be found, such as microwave invisible solar panels and stealth windows [18], [19]. Some optically transparent designs adopted air gaps and complementary layers to increase absorption bandwidth with angular stability [16], [20]. It should be noted that few absorber designs focused on extended absorption (above 95%) in a wideband [21]. Yet, this is a critical design metric for stealth airplane canopies together with high optical transparency. Nevertheless, designing an optically transparent single-layer metamaterial absorber that consists of unit cells without air gaps and complementary layers, while satisfying polarization insensitivity and robust performance under oblique incidence with wideband over 95% absorption has not been reported to date.

This letter proposes and demonstrates an optically transparent thin absorber with over 90% absorption in the frequency band of 4.4 GHz to 11.2 GHz, and impressively, approximately 95% absorption between 4.8 GHz and 10.6 GHz. The absorber is insensitive to all polarization angles and shows more than 90% absorption for incident angles up to 40° for transverse electric (TE) and up to 60° for transverse magnetic (TM) polarizations in the frequency range of 4.4 GHz to 11.2 GHz. We fabricated a prototype, and due to its inherent characteristic of single-layer dielectric design combined with the same indium-tin-oxide

Received 30 December 2024; revised 25 February 2025; accepted 28 April 2025. Date of publication 12 May 2025; date of current version 6 August 2025. This work was supported by the Scientific and Technological Research Council of Türkiye (TUBITAK) under Grant 20AG001. *(Corresponding author: Furkan Şahin.)*

Furkan Şahin was with the Department of Electrical and Electronics Engineering, Bilkent University, Ankara 06800, Türkiye, and also with the National Institute of Materials Science and Nanotechnology (UNAM), Bilkent University, Ankara 06800, Türkiye. He is now with Eindhoven University of Technology, 5612 Eindhoven, The Netherlands (e-mail: fshn97@gmail.com).

Emre Ünal is with the Department of Electrical and Electronics Engineering, Bilkent University, Ankara 06800, Türkiye, and also with the National Institute of Materials Science and Nanotechnology (UNAM), Bilkent University, Ankara 06800, Türkiye (e-mail: unale@bilkent.edu.tr).

Vakur B. Ertürk is with the Department of Electrical and Electronics Engineering, Bilkent University, Ankara 06800, Türkiye (e-mail: vakur@ee.bilkent.edu.tr).

Hilmi Volkan Demir is with the Department of Electrical and Electronics Engineering, Bilkent University, Ankara 06800, Türkiye, also with the National Institute of Materials Science and Nanotechnology (UNAM), Bilkent University, Ankara 06800, Türkiye, also with the Department of Physics, Bilkent University, Ankara 06800, Türkiye, and also with the School of Electrical and Electronic Engineering and the School of Physical and Mathematical Sciences, Nanyang Technological University,, Singapore 639798 (e-mail: volkan@bilkent.edu.tr).

Digital Object Identifier 10.1109/LAWP.2025.3568924

(ITO) sheets, fabrication complexity and costs are reduced. We tested proof-of-concept fabricated absorbers and found that absorption measurements are in agreement with the numerical predictions.

II. Design and Analysis

The proposed absorber is designed by using polymethyl methacrylate (PMMA) ($\epsilon_r = 2.8$ and $\tan_\delta = 0.02$) as a dielectric layer and two ITO layers with 16 Ω/sq sheet resistance. The first ITO layer forms the ground layer and ensures zero transmission at the RF band. The second ITO layer has a unique pattern on top of the dielectric layer. Altogether, the whole design allows broad absorption in RF frequencies. The dimensions of the pattern layer are obtained with a methodology explained in the following section.

A. Initial Absorber Geometry

To begin with, a single square loop (SSL) unit cell design was considered as the initial design due to its simplicity, extensive use in literature, and availability for pixelated designs. Yet, SSL unit cell-based absorbers can provide narrowband absorption [22]. This SSL design was optimized, and above 90% absorption was only achieved between 3.8 GHz and 5.0 GHz that can be considered as narrow band. Apart from this design, four small SSLs placed in the corners of the same unit cell were considered as an alternative. This design was also optimized, and above 90% absorption was achieved between 7.0 GHz and 10.0 GHz. In the end, these two designs were combined, as shown in Fig. 1(a), to achieve a wideband absorption.

B. Final Absorber Geometry

The initial design achieved a relatively wideband absorption, as shown in Fig. 2. Then, particle swarm optimization (PSO) was used to further optimize the absorption spectra. First, the sheet resistance of ITO films, permittivity of dielectric layer, and the height of the substrate layer were fixed due to the materials available at our hand. Since the bottom ITO film has no patterned shape, optimization was applied only to the geometry of the top layer.

First, considering the symmetry, only the part of the unit cell in the first octant of the Cartesian plane was used in the optimization process. After taking the first octant's vertical, horizontal, and diagonal symmetries, whole unit cell design was determined. Thus, polarization insensitivity of the design was ensured by utilizing fourfold rotational symmetry similar to that explained in [23]. Then, the first octant of the unit cell was converted to pixels with a value of 1's corresponding to the presence of ITO or otherwise 0's corresponding to the absence of ITO. Then, the unit cell was considered as 64 × 64 pixels by considering the compromise between the resolution and simulation time. Furthermore, only one-eighth of the total pixels was used due to the aforementioned fourfold symmetry condition. PSO was used on the pixel values while taking the initial absorber geometry as a basis. This was achieved by constraining some of the geometric dimensions of the initial design. Furthermore, only reflection values are checked, thanks to the ground plane. Thus, the required amount of simulation time to reach optimum

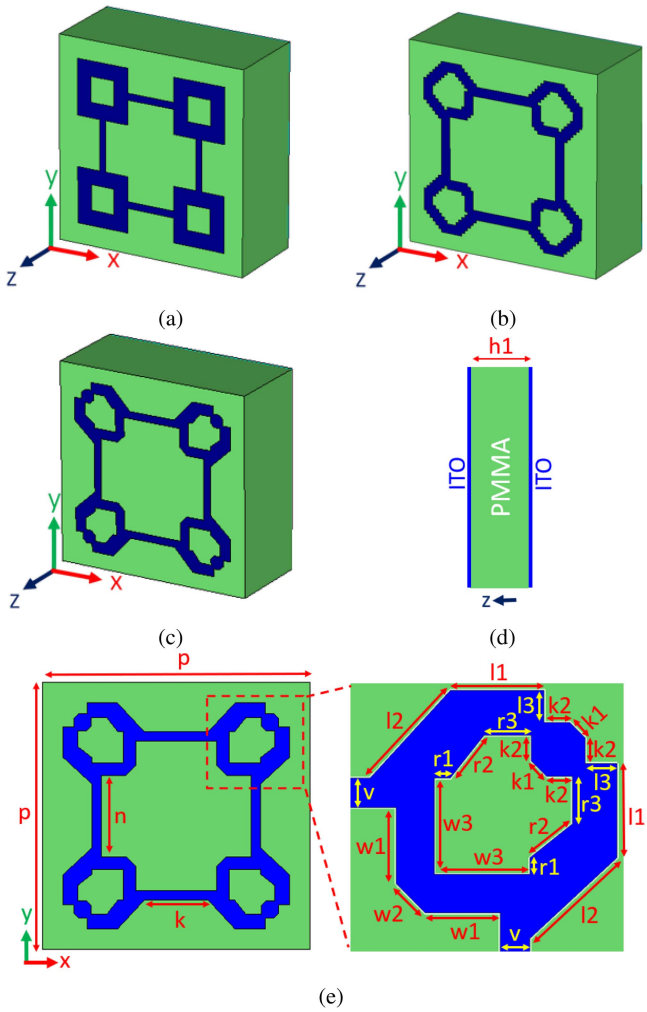

Fig. 1. Perspective view of the (a) initial, (b) first optimized, and (c) FD of the proposed absorber. (d) Side view and (e) top view of the FD. (a) Initial design. (b) FOD. (c) FD. (d) Side view. (e) Single unit cell with dimensions.

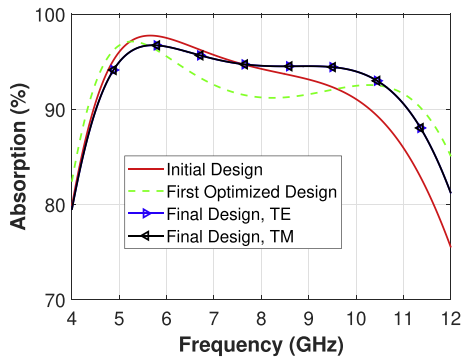

Fig. 2. Simulated absorption results of initial, first optimized and FDs for TE and TM polarizations.

design was reduced significantly. Then, the optimization goal was decided based on the lowest thickness in terms of the longest operating wavelength and fractional bandwidth (FB). On the basis of the literature overview of single-layer optically transparent absorbers, we decided on our termination criterion. Thus, we targeted a thickness less than $0.08\lambda_L$ and above 90% FB. We chose the design that satisfies the desired performance metrics as the first optimized design (FOD) after 500 iterations. Each iteration takes approximately 65 s using a computer that

TABLE I
FB COMPARISON OF FOD AND FD

	≥ 90% Absorption FB (%)	≥ 95% Absorption FB (%)
FOD	91.1	34.2
FD	87.2	69.4

has i7 processor. The geometry and absorption spectra are shown in Figs. 1(b) and 2, respectively.

As shown in Fig. 2, FOD has an absorption response that barely exceeds 90% in a specific frequency range. Even if this design yields the highest absorption bandwidth, it is possible to encounter less than 90% absorption due to possible manufacturing problems of the fabricated prototype. Then, we used another PSO goal for the FOD by targeting 95% absorption FB, which is also a requirement for stealth canopy applications while still satisfying less than $0.08\lambda_L$ thickness. Table I shows the comparison of the performance metrics of these two designs. The results indicate that the final design (FD) outperforms the FOD for 95% absorption FB without sacrificing 90% absorption FB. The final geometry is given in Fig. 1(c)–(e) with dimensions in mm as h1 = 5.0, h2 = 0.2 (thickness of ITO layer), p = 12, n = 3.65, k = 2.89, v = 0, w1 = 1.11, w2 = 0.6, w3 = 1.4, r1 = 0.24, r2 = 0.77, r3 = 0.69, l1 = 1.375, l2 = 1.74, l3 = 0.47, k1 = 0.32, and k2 = 0.375. Last, polarization insensitivity can be observed for TE and TM polarizations in Fig. 2.

C. Simulation Results for Oblique Incidence Case

The proposed absorber is simulated using CST Microwave Studio. In CST, unit cell boundary conditions and Floquet port excitation are used. Only two modes of Floquet port were propagating in the medium. We considered only reflection to analyze absorption due to negligible transmission values and thus, T(ω) = 0 (i.e., $|S_{21}|^2$ is ignored in the following):

$$A(\omega) = 1 - R(\omega) - T(\omega) = 1 - |S_{11}|^2 - |S_{21}|^2. \quad (1)$$

We analyzed the absorption response for different incidence angles. Absorption graphs are different for TE and TM polarized waves, as given in Fig. 3. Absorption is higher than 90% for angles up to 40° for TE polarization, as shown in Fig. 3(a). Lower absorption values are observed since the reflected and multirefracted waves increase with larger incidence angles [24]. However, absorption remains higher than 90% even for 60° incident angle in TM polarization with a shift to higher frequencies, as presented in Fig. 3(b). Furthermore, simulated surface currents for resonance frequencies are given in Fig. 4(a) and (b). Less surface current density observed at higher frequencies similar to the other designs is available in literature [25].

III. FABRICATION AND MEASUREMENTS

The patterned and ground layers are comprised of ITO coated on 100 μm thick polyethylene terephthalate sheets. Since the ground layer has no pattern, only the patterned layer was etched using a 355 nm laser source. Due to scan area limits, an 8 cm × 8 cm area was etched each time. After the etching process was finished for a particular area, the sample was moved using linear stages. In the end, the total area of 20 cm × 20 cm was processed. After the etching, the top and ground layers were attached to PMMA with transparent glue. The fabricated prototype is shown in Fig. 5(a). A small piece of the prototype (3 cm × 3 cm) was also fabricated and was placed inside Cary 60 UV-Vis spectrophotometer, as shown in Fig. 5(b). In total, 65% average optical transmittance was found for the visible wavelengths, as given in Fig. 5(c).

After the fabrication step, measurements were taken under normal and oblique incidence conditions. First, a pair of double ridge horn antennas were connected to the Keysight E5063 A Vector Network Analyzer. These antennas have an operating frequency range that is covering 3 GHz to 12 GHz. Then, the fabricated absorber and antennas were positioned based on the intended normal and oblique incidence angle. The setup is shown in the Fig. 5(d). First, normal incidence case was measured

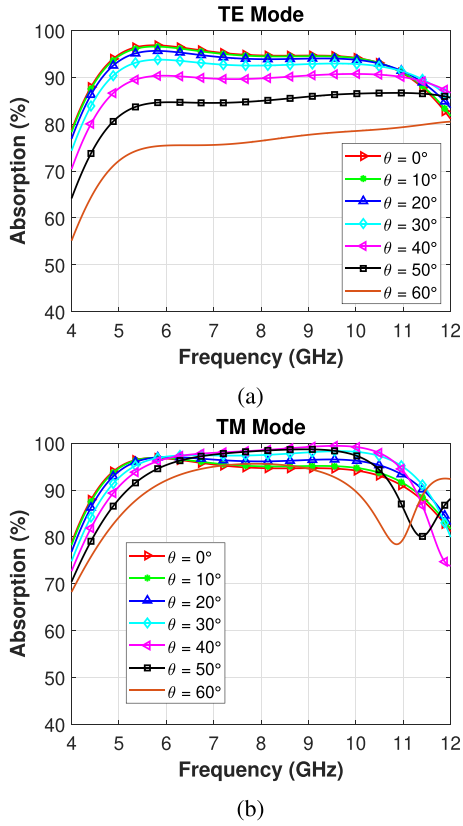

Fig. 3. Simulated absorption spectra under different oblique incidence angles for (a) TE and (b) TM polarizations.

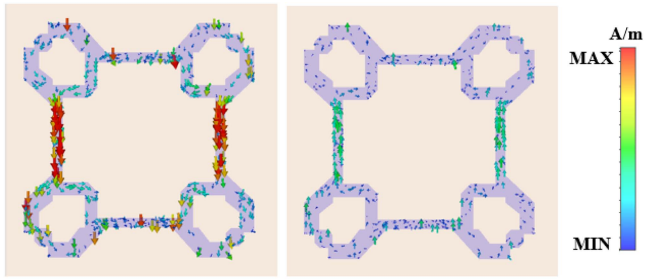

Fig. 4. Simulated surface current density for resonance frequencies at (a) 5.6 GHz and (b) 9.3 GHz.

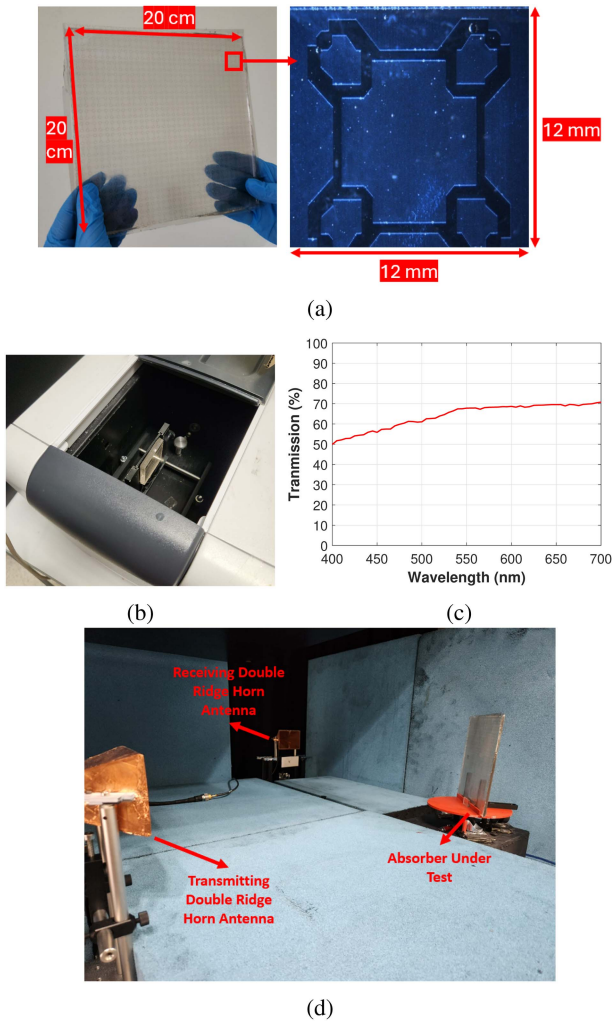

Fig. 5. Images of the (a) fabricated prototype and one unit cell under optical microscope and (b) optical spectrophotometer and small prototype placed inside. (c) Optical transmission spectrum across the visible wavelengths. (d) Microwave free-space measurement setup with antennas and absorber.

TABLE II
COMPARISON WITH OTHER OPTICALLY TRANSPARENT SINGLE-LAYER METAMATERIAL ABSORBERS

Ref.	$\geq$ 90% Abs. FB (%)	Thickness (λ_L)	Incident Angle
[18]	74.7	0.093	45° TE, 40° TM
[26]	44.6	0.08	45° TE, 70° TM
[27]	71.2	0.08	30° TE, 60° TM
[28]	65.7	0.092	45° TE, 45° TM
[29]	88.5	0.196	40° TE, 60° TM
This work	87.2	0.079	40° TE, 60° TM

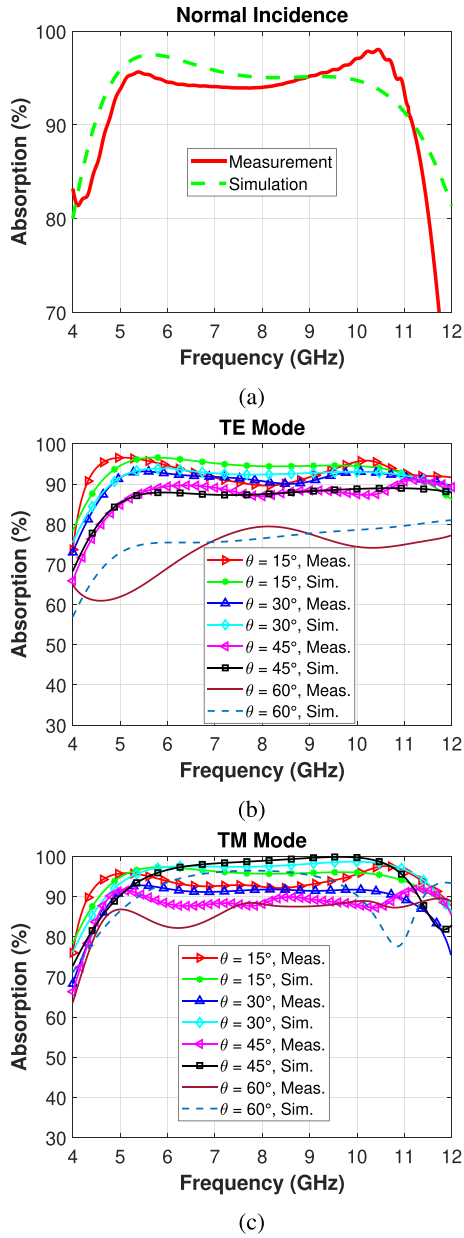

Fig. 6. Experimentally measured absorption spectra together with simulation results under (a) normal incidence, and (b) and (c) different oblique incidence angles for TE and TM polarizations, respectively.

using a single antenna. An excellent validation of simulation results was observed and results were presented in Fig. 6(a). The measurements were repeated for TE and TM polarizations and compared with simulations as shown in Fig. 6(b) and (c), respectively. We obtained good agreement between the measurement and simulation results up to 45° oblique incidence. In addition, constructive and destructive edge scattering from the fabricated prototype may have resulted in some deviations. Table II compares our fabricated absorber with other designs available in the literature, where our design outperforms in terms of FB, thickness in terms of the largest operating wavelength, and performance under different oblique incidence angles.

IV. CONCLUSION

We proposed and demonstrated an extremely thin optically transparent metamaterial absorber that works in the 4.8 GHz to 10.6 GHz frequency band with more than 95% absorption and remarkable transparency in the optical regime. In the same band, the proposed design exhibits more than 90% absorption for incident angles up to 40° for TE and 60° for TM polarizations. This absorber design presented that optical transparency, small thickness, and sufficiently invariant performance for oblique incident angles are achievable using a single dielectric layer without sacrificing mechanical robustness with air gaps and increasing fabrication complexity using multiple layers.

REFERENCES

[1] W. Li, M. Xu, H. Xu, X. Wang, and W. Huang, "Metamaterial absorbers: From tunable surface to structural transformation," *Adv. Mater.*, vol. 34, no. 38, 2022, Art. no. 2202509.

[2] P. Garg and P. Jain, "A review of metamaterial absorbers and their application in sensors and radar cross-section reduction," *Microw. Opt. Technol. Lett.*, vol. 65, no. 2, pp. 387–411, 2022.

[3] H. Xiong, J.-S. Hong, C.-M. Luo, and L.-L. Zhong, "An ultrathin and broadband metamaterial absorber using multi-layer structures," *J. Appl. Phys.*, vol. 114, no. 6, 2013, Art. no. 064109.

[4] L. Li and Z. Lv, "Ultra-wideband polarization-insensitive and wide-angle thin absorber based on resistive metasurfaces with three resonant modes," *J. Appl. Phys.*, vol. 122, no. 5, 2017, Art. no. 055104.

[5] H. Luo, Y. Z. Cheng, and R. Z. Gong, "Numerical study of metamaterial absorber and extending absorbance bandwidth based on multi-square patches," *Eur. Phys. J. B.*, vol. 81, no. 4, pp. 387–392, 2011.

[6] L. Li et al., "A band enhanced metamaterial absorber based on e-shaped all-dielectric resonators," *AIP Adv.*, vol. 5, no. 1, 2015, Art. no. 017147.

[7] S. Li et al., "Wideband, thin, and polarization-insensitive perfect absorber based the double octagonal rings metamaterials and lumped resistances," *J. Appl. Phys.*, vol. 116, no. 4, 2014, Art. no. 043710.

[8] P. Munaga, S. Ghosh, S. Bhattacharyya, and K.V. Srivastava, "A fractal-based compact broadband polarization insensitive metamaterial absorber using lumped resistors," *Microw. Opt. Technol. Lett.*, vol. 58, no. 2, pp. 343–347, 2015.

[9] S. Fan and Y. Song, "Bandwidth-enhanced polarization-insensitive metamaterial absorber based on fractal structures," *J. Appl. Phys.*, vol. 123, no. 8, 2018, Art. no. 085110.

[10] S. Ghosh, S. Bhattacharyya, Y. Kaiprath, and K. V. Srivastava, "Bandwidth-enhanced polarization-insensitive microwave metamaterial absorber and its equivalent circuit model," *J. Appl. Phys.*, vol. 115, no. 10, 2014, Art. no. 104503.

[11] Q. Huang et al., "Metamaterial electromagnetic wave absorbers and devices: Design and 3D microarchitecture," *J. Mater. Sci. Technol.*, vol. 108, pp. 90–101, 2022.

[12] B. Munk, *Frequency Selective Surfaces: Theory and Design*. New York, NY, USA: Wiley, 2000.

[13] P. Ranjan, A. Choubey, S. K. Mahto, and R. Sinha, "A six-band ultra-thin polarization-insensitive pixelated metamaterial absorber using a novel binary wind driven optimization algorithm," *J. Electromagn. Waves Appl.*, vol. 32, no. 18, pp. 2367–2385, 2018.

[14] A. Dimitriadis, N. Kantartzis, and T. Tsiboukis, "A polarization-/angle-insensitive, bandwidth-optimized, metamaterial absorber in the microwave regime," *Appl. Phys. A.*, vol. 109, no. 4, pp. 1065–1070, 2012.

[15] B. Bian et al., "Novel triple-band polarization-insensitive wide-angle ultra-thin microwave metamaterial absorber," *J. Appl. Phys.*, vol. 114, no. 19, 2013, Art. no. 194511.

[16] A. Bhardwaj, G. Singh, K.V. Srivastava, J. Ramkumar, and S. A. Ramakrishna, "Polarization-insensitive optically transparent microwave metamaterial absorber using a complementary layer," *IEEE Antennas Wireless Propag. Lett.*, vol. 21, no. 1, pp. 163–167, Jan. 2022.

[17] H. Jiang et al., "A conformal metamaterial-based optically transparent microwave absorber with high angular stability," *IEEE Antennas Wireless Propag. Lett.*, vol. 20, no. 8, pp. 1399–1403, Aug. 2021.

[18] S. Li et al., "Ultrathin optically transparent metamaterial absorber for broadband microwave invisibility of solar panels," *J. Phys. D: Appl. Phys.*, vol. 55, no. 4, 2021, Art. no. 045101.

[19] H. Xiao et al., "Optically transparent broadband and polarization insensitive microwave metamaterial absorber," *J. Appl. Phys.*, vol. 126, no. 13, 2019, Art. no. 135107.

[20] T. Li et al., "Optically transparent metasurface Salisbury screen with wideband microwave absorption," *Opt. Exp.*, vol. 26, no. 26, Dec. 2018, Art. no. 34384.

[21] S. Liu, F. Ding, J. Wu, Q. Zhang, and H. Yang, "A metamaterial absorber with centre-spin design and characteristic modes analysis," *Physica Scripta*, vol. 97, no. 4, Mar. 2022, Art. no. 045502.

[22] M. I. Hossain, N. Nguyen-Trong, K. H. Sayidmarie, and A. M. Abbosh, "Equivalent circuit design method for wideband nonmagnetic absorbers at low microwave frequencies," *IEEE Trans. Antennas Propag.*, vol. 68, no. 12, pp. 8215–8220, Dec. 2020.

[23] C. M. Watts, X. Liu, and W. J. Padilla, "Metamaterial electromagnetic wave absorbers," *Adv. Mater.*, vol. 24, no. 23, pp. OP98–OP120, May 2012.

[24] S.-J. Li et al., "Analysis and design of three-layer perfect metamaterial-inspired absorber based on double split-serration-rings structure," *IEEE Trans. Antennas Propag.*, vol. 63, no. 11, pp. 5155–5160, Nov. 2015.

[25] M. D. Banadaki, A. A. Heidari, and M. Nakhkash, "A metamaterial absorber with a new compact unit cell," *IEEE Antennas Wireless Propag. Lett.*, vol. 17, no. 2, pp. 205–208, Feb. 2018.

[26] S. Li et al., "Ultrathin optically transparent electromagnetic shielding window with broadband microwave absorption and ultrahigh optical transmittance," *Int. J. RF Microw. Comput.-Aided Eng.*, vol. 32, no. 11, 2022, Art. no. e23338.

[27] Y. Xiong, F. Chen, Y. Cheng, and H. Luo, "Ultra-thin optically transparent broadband microwave metamaterial absorber based on indium tin oxide," *Opt. Mater.*, vol. 132, 2022, Art. no. 112745.

[28] M. Suo, H. Xiong, X.-K. Li, Q.-F. Liu, and H.-Q. Zhang, "A flexible transparent absorber bandwidth expansion design based on characteristic modes," *Results Phys.*, vol. 46, 2023, Art. no. 106265.

[29] Y. Tayde et al., "An optically transparent and flexible microwave absorber for X and Ku bands application," *Microw. Opt. Technol. Lett.*, vol. 62, no. 5, pp. 1850–1859, Jan. 2020.